15TH IEA HEAT PUMP CONFERENCE
MAY 26–29, 2026 | HOFBURG
VIENNA 2026
DECARBONISATION THROUGH INNOVATION

# Investigation method for the icing behavior on coated surfaces of evaporators in air-source heat pumps

Julian Deufel[a,b,*], Peter Stein[b], Heimo Walter[a]

[a]Institute for Energy Systems and Thermodynamics, TU Wien, Getreidemarkt 9/302, Vienna A-1060, Austria
[b]University of Applied Sciences Konstanz, Alfred-Wachtel-Straße 8, Konstanz D-78462, Germany

**Abstract**

Heat pumps are considered a key technology in the energy transition and have become widely used in the building sector in recent years. However, under real operating conditions the evaporators of air-source heat pumps (ASHP) are often exposed to icing, particularly at low ambient temperatures. When the surface temperature of the evaporator drops below the dew point, water vapor from the air condenses and freezes on the surface. This ice formation impairs system performance and energy efficiency by increasing flow resistance and reducing heat transfer. To mitigate these effects, various functional coatings have been developed to influence wetting and icing behavior. Despite the increasing availability of such anti-icing coatings, a systematic and reproducible method for their comparative evaluation under realistic ASHP operating conditions is still lacking. This paper presents an experimental investigation methodology that enables a quantitative and reproducible analysis of the icing behavior of coated evaporator surfaces. The method combines thermodynamic measurements with image-based evaluation to characterize frost formation and detachment. Dedicated test rigs operated in a controlled climate chamber allow precise adjustment of temperature, humidity, and airflow. The modular test design enables targeted analysis of individual icing and defrosting processes and supports the assessment of different coatings. The proposed methodology thus provides a resource-efficient and practical approach for identifying suitable coating candidates for real evaporator geometries and contributes to the development of more efficient and reliable heat pump systems.



*Keywords: air source heat pump; frosting; icephobic; test method; evaporator*

## 1. Introduction

Heat pump technologies are increasingly becoming an essential component of energy-efficient heating and cooling systems and are widely used, particularly in the field of room air conditioning. A heat pump operates according to a reversed Carnot cycle. In this process thermal energy is extracted from a low-temperature reservoir and transferred to a higher temperature level to provide heating for indoor spaces.

At low ambient temperatures, when the dew point temperature is undershot, water vapor contained in the air condenses on the surface of the evaporator. Consequently, frost or ice layers form on the surface [1–3]. This ice formation has a negative impact on the operation of the heat pump, reducing both heat transfer and airflow through the evaporator [4–8]. The increasing flow resistance and decreasing heat transfer efficiency eventually lead to inefficient operation, making it necessary to initiate a defrost cycle to remove the accumulated ice.

Various defrosting strategies have been reported in the literature [9-10], with reverse-cycle defrosting being the most commonly applied commercial solution [11]. In this process, the refrigerant cycle is reversed so that energy is transferred from the heated indoor environment back to the evaporator. However, this method is associated with a reduction in system efficiency, since not only is heat withdrawn from the indoor space, but

* Corresponding author. Tel.: +49-7531-206-670
*E-mail address:* jdeufel@htwg-konstanz.de

additional compressor energy is also required. Furthermore, in many systems, heating operation is interrupted during the defrost cycle, which further affects overall performance. For this reason, ongoing research focuses on reducing the frequency and duration of defrosting cycles or avoiding them altogether [12-13].

A promising approach is to prevent or delay ice formation on the evaporator surface. To achieve this, both micro- and nanostructured surfaces [14-15] and functional surface coatings [7,16-17] have been investigated. The combination of these approaches shows additional potential for a sustained long-term reduction in frost accumulation [18]. However, a systematic comparison of different coatings with respect to their icing behavior under realistic operating conditions is still lacking.

In this paper, an experimental analysis method will be presented, which allows a quantitative and reproducible investigation of the icing behavior of a (coated) heat exchanger. The suitability of the method will be demonstrated by means of an experimental investigation. Based on the obtained results, a selection of promising coatings can be identified for application on evaporator surfaces, aiming to improve the icing and defrosting behavior of heat pumps in the long term.

## 2. Methods

The application of heat exchangers in heat pumps requires specific properties in the evaporator material. It must combine high thermal conductivity, long-term durability, and resistance to environmental influences. Any measures to improve icing behavior must therefore not adversely affect key thermodynamic properties, especially thermal conductivity. To characterize the material's frosting and defrosting behavior, experimental investigations are conducted to assess the rate of ice formation, the adhesion strength between ice and the surface, and the efficiency of ice removal during defrosting. This approach enables the identification of suitable coatings. Similar to Leoni et al. [19], the initial investigations were carried out on geometrically simple aluminum samples (50 mm × 200 mm × 1 mm) due to the complexity of the icing process and the large number of coating variations. All experiments were conducted in a temperature- and humidity-controlled climate chamber (Vötsch VC³ 7034).

### *2.1. Surface icing evaluation*

A qualitative evaluation of the icing behavior was first conducted to identify coatings with visually reduced frost formation. The aluminum samples (50 mm × 200 mm × 1 mm) were divided into four equal sections, three of which were coated with different materials, while the fourth remained uncoated and served as a reference. The samples are mounted on a test rig (see Fig. 1(a)) equipped with three identical Peltier elements (Quick-Cool QC-71-1.4-8.5M) on the underside. Heat transfer pads (Keratherm Softtherm 86/600) ensure uniform thermal contact between the Peltier modules and the sample surface. The samples are fixed using toggle clamps, and Type-K thermocouples are placed between them to measure the surface temperature.

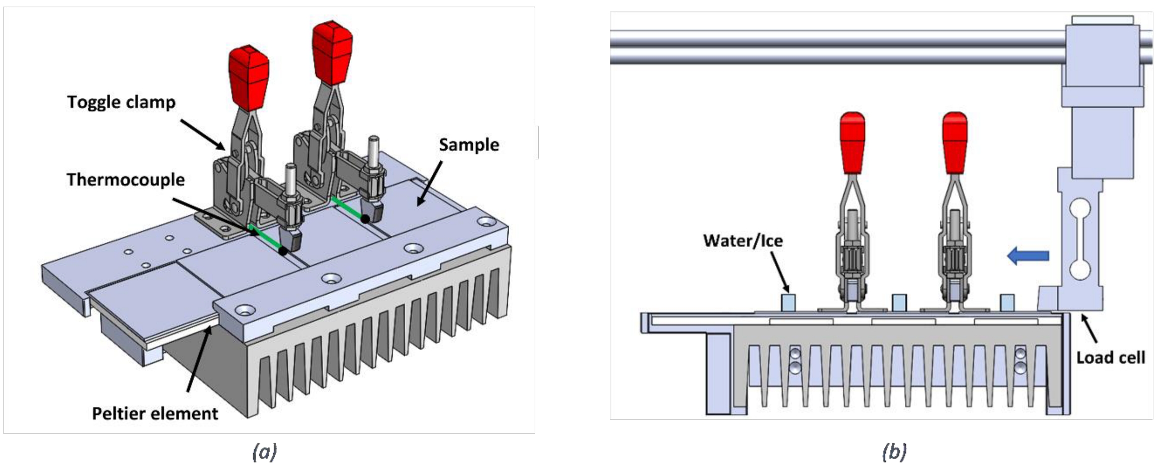


Figure 1. Different experimental setups: (a) surface icing and (b) ice adhesion

The setup is placed inside the climate chamber, where the temperature (5 °C) and relative humidity (≈90 %) are kept constant. Both parameters are monitored using the chamber control system and an additional climate sensor (Testo 480). Once the environmental conditions stabilize, the surface temperature is lowered to –15 °C via the Peltier elements. The icing process is recorded using a camera installed in the chamber. When all surface areas are fully covered by ice (after approximately 15 minutes), the test is completed.

*2.2. Measurement of ice adhesion*

The adhesion strength of ice on the coated surfaces is determined using a horizontal push test [20–22]. A force sensor mounted on a lead screw mechanism is moved across the surface at a constant distance of 1 ± 0.2 mm, pushing against frozen ice cylinders shown in Fig. 1(b).

Cylindrical polyamide tubes with an inner diameter of 4 mm are used as molds. Once the chamber and samples reached the target conditions (5 °C and ≈50 % relative humidity (RH)), 0.05 ml of water is pipetted into each tube. The samples are then cooled rapidly in multiple test runs to different target temperatures (–3, –7, –10, –15 °C), causing the water to freeze. The peak force measured during the push test and the average value are used to determine the adhesive shear strength.

*2.3. Icing under forced convection*

Evaporators in real operation are continuously exposed to an airflow due to the built-in fan, so the icing behavior under forced convection must also be investigated. An axial suction fan directs airflow through a duct across the samples. For this test, the coatings are reapplied on new aluminum plates of identical dimensions, each with a single coating to ensure higher application quality and reproducibility.

To enhance comparability, a cooling plate with four positions is designed. It is temperature-controlled by a circulating coolant (PEKASOL L) supplied from a thermostat (Julabo Dyneo DD-1200F). The chamber conditions are maintained at 5 °C and ≈90 % RH, with an airflow velocity of approximately 2 m/s. The icing process is recorded using a camera for visual comparison of the coatings.

*2.4. Evaluation on a heat exchanger model*

Based on the results of the preliminary tests, selected coatings are applied to a heat exchanger (Fig. 2(b)) to assess their performance under near-operational conditions. The heat exchanger is thermally controlled by the same external chiller system as in the preliminary tests. It consists of multiple copper tubes (10 mm x 1 mm) equipped with aluminum fins (170 mm x 50 mm x 1 mm), which are mounted via fitted holes. The overall configuration is similar to the design described by Yang et al. [23]. Copper sleeves (12 mm x 1 mm x 5 mm) with the same inner diameter as the outer diameter of the pipe are inserted between the fins to adjust and fix the fin spacing (Fig. 2(a)).

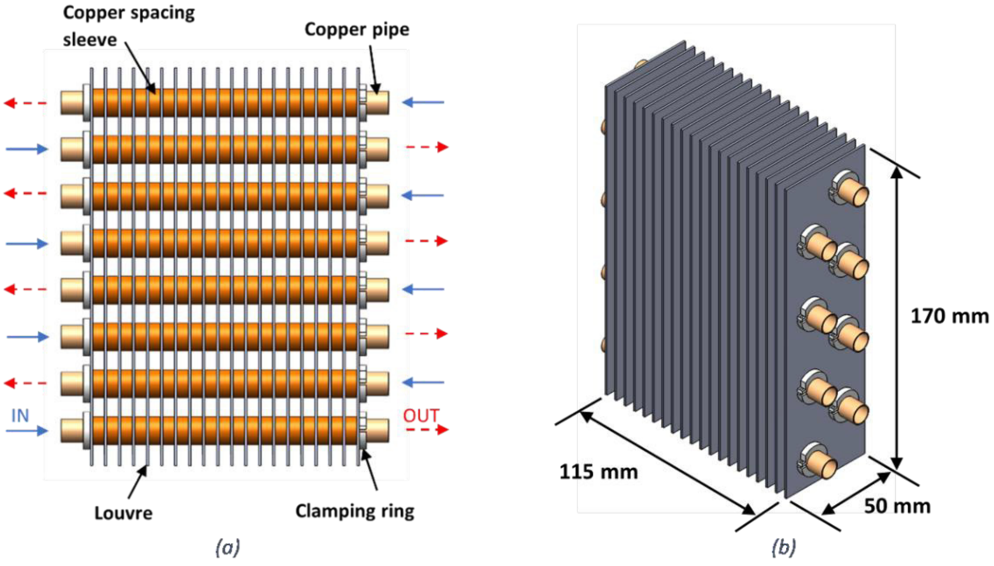


Figure 2. (a) Structure of the heat exchanger model with the pipe flows and the (b) dimensions

The fin package is mechanically preloaded using clamping rings at both ends to ensure proper thermal contact and prevent deformation during icing.

Unlike in a real heat pump, no evaporating refrigerant is used in this setup. Instead, a liquid coolant is circulated through the system. In a single flow path, the temperature gradient between inlet and outlet would be too high. To avoid this, the inlet flow is split into two streams and further distributed by a flow distributor into four parallel channels on each side, ensuring uniform flow distribution across the heat exchanger. The two flow directions are arranged counter-currently to minimize temperature gradients along the fins.

The mass flow rate and fluid temperature are measured at the inlet and outlet of the main (undivided) flow paths using magnetic-inductive flow sensors (ifm SM6120). The transferred heat is calculated from the temperature difference and mass flow rate, and the cumulative heat uptake is determined over time for comparison between coatings. Four Type-K thermocouples are attached to the fin surfaces to monitor temperature. An adjustable axial suction fan mounted at the rear of the heat exchanger provides the required airflow through the fin package and allows variable speed control. For defrosting, the airflow direction can be reversed.

At the beginning of each test, the chamber temperature (3 °C, ≈90 % RH) and coolant temperature (-15 °C) are stabilized. Once steady-state conditions are achieved, the coolant flow is initiated, and the fan is switched on. During defrosting, the coolant circulation is stopped, and the coolant is heated. Once the coolant reaches 10 °C, the circuit is reopened and the heat exchanger is completely defrosted. A front-mounted camera records the entire test sequence for subsequent evaluation.

## 3. Results and Discussion

The setup of the basic surface icing experiment with an uncoated aluminum sample is shown in Fig. 3(b). The progressive formation of ice on the sample surface over time can be clearly observed. Fig. 3(a) shows the force signal recorded during one run of the push test at a surface temperature of -10 °C. Each peak corresponds to the detachment of a single ice cylinder from the surface. The measurements show reproducible results with a deviation of around ±10 %. From the measured forces, the ice adhesion strength is derived, which ranges between 1100 and 1300 kPa and is consistent with values reported in the literature. The observed scatter also corresponds well to published data [22]. Obvious measurement errors, such as the fourth peak in Fig. 3(a), are excluded from the evaluation.

Fig. 3(c) presents a section of the optical sequence during the icing of the bare aluminum heat exchanger. A homogeneous and evenly distributed frost layer forms across the entire surface. In addition, the figure shows the development of the cumulative absorbed heat during the freezing and defrosting phases, based on three identical measurements (n = 3). To calculate the absorbed heat, the enthalpy flow rates at the inlet and outlet were determined, taking into account the temperature dependence of the specific heat capacity and the density of the coolant. The statistical (Type A) uncertainty of the mean was evaluated in accordance with ISO/IEC Guide 98-3 (GUM). For the frosting cycle, a value of 0.533 ± 0.002 kWh was obtained, while for the defrosting cycle 0.056 ± 0.0003 kWh was determined.

The conducted experiments enable a qualitative and quantitative assessment of heat exchanger performance under various operating conditions. The experimental setup allows the determination of the energy absorbed during heating operation and the energy required during the defrosting process. For the uncoated heat exchanger, it is observed that the energy demand of the defrosting process accounts for approximately 10 % of the heating operation.

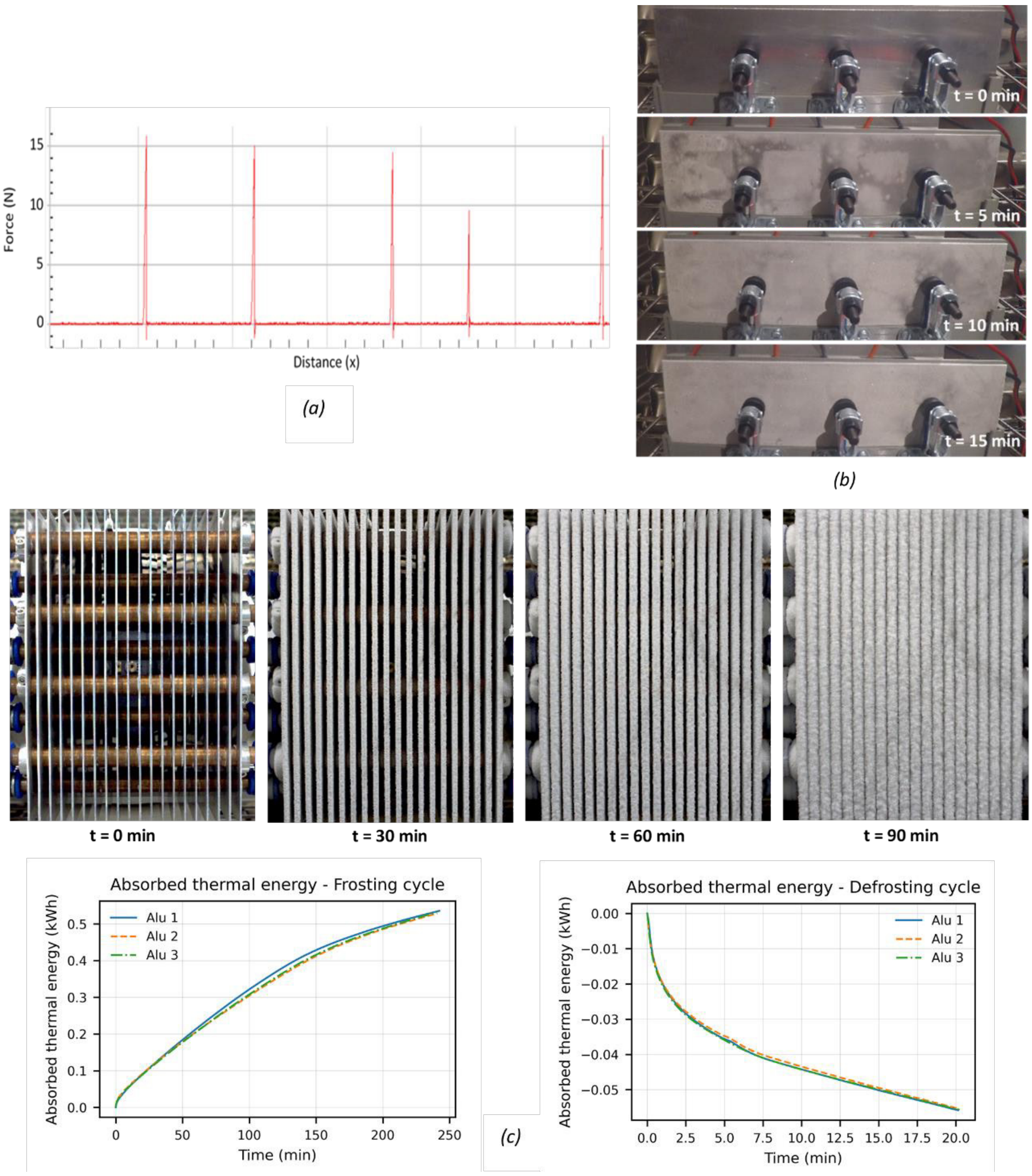


Figure 3. Results of the experiment: (a) force measurement on ice adhesion gauge, (b) progress of the icing test and (c) image capture and energy curve during frosting and defrosting of the heat exchanger

## 4. Conclusion

The presented methodology provides a practical and reproducible approach for the comparative evaluation of different materials and their icing behavior. Using the developed testing methodology based on simple aluminum samples, the material and experimental effort can be kept low while enabling a reliable selection of promising coatings. Considering the growing availability of such coatings, the approach enables an initial assessment of their suitability for heat pump applications and serves as a basis for future studies under realistic operating conditions. Further work will include cyclic operation tests with alternating heating and defrost phases to evaluate the influence on the seasonal performance factor and long-term system efficiency.

## Acknowledgements

This work was funded by the program Invest BW - Innovation III (Grant No.: BW1_4082/02).

**References**


[1] Wu X, Dai W, Xu W, Tang L. Mesoscale investigation of frost formation on a cold surface. Experimental Thermal and Fluid Science 2007;31:1043–8.

[2] Zhang Y, Zhang G, Zhang A, Jin Y, Ru R, Tian M. Frosting Phenomenon and Frost-Free Technology of Outdoor Air Heat Exchanger for an Air-Source Heat Pump System in China: An Analysis and Review. Energies 2018;11:2642

[3] Na B, Webb RL. A fundamental understanding of factors affecting frost nucleation. International Journal of Heat and Mass Transfer 2003;46:3797–808.

[4] Boyina KS, Mahvi AJ, Chavan S, Park D, Kumar K, Lira M, et al. Condensation frosting on meter-scale superhydrophobic and superhydrophilic heat exchangers. International Journal of Heat and Mass Transfer 2019;145:118694.

[5] Guo X-M, Chen Y-G, Wang W-H, Chen C-Z. Experimental study on frost growth and dynamic performance of air source heat pump system. Applied Thermal Engineering 2008;28:2267–78.

[6] Wang F, Liang C, Yang M, Fan C, Zhang X. Effects of surface characteristic on frosting and defrosting behaviors of fin-tube heat exchangers. Applied Thermal Engineering 2015;75:1126–32.

[7] Moallem E, Cremaschi L, Fisher DE, Padhmanabhan S. Experimental measurements of the surface coating and water retention effects on frosting performance of microchannel heat exchangers for heat pump systems. Experimental Thermal and Fluid Science 2012;39:176–88.

[8] Huang D, Ri-Jing Z, Liu Y, Yi D-B. Effect of fin types of outdoor fan-supplied finned-tube heat exchanger on periodic frosting and defrosting performance of a residential air-source heat pump. Applied Thermal Engineering 2014;69:251–60.

[9] Ma L, Sun Y, Wang F, Wang M, Zhang S, Wang Z. Advancements in anti-frosting and defrosting techniques for air source heat pumps: A comprehensive review of recent progress. Applied Energy 2025;377:124358.

[10] Song M, Deng S, Dang C, Mao N, Wang Z. Review on improvement for air source heat pump units during frosting and defrosting. Applied Energy 2018;211:1150–70.

[11] Dong J, Deng S, Jiang Y, Xia L, Yao Y. An experimental study on defrosting heat supplies and energy consumptions during a reverse cycle defrost operation for an air source heat pump. Applied Thermal Engineering 2012;37:380–7.

[12] Liang C, Li X, Meng X, Shi W, Gu J, Wang B, et al. Experimental investigation of heating performance of air source heat pump with stable heating capacity during defrosting. Applied Thermal Engineering 2023;235:121433.

[13] Jang JY, Bae HH, Lee SJ, Ha MY. Continuous heating of an air-source heat pump during defrosting and improvement of energy efficiency. Applied Energy 2013;110:9–16.

[14] Fürbacher R, Grünsteidl G, Otto A, Liedl G. Chemical and UV Durability of Hydrophobic and Icephobic Surface Layers on Femtosecond Laser Structured Stainless Steel. Coatings 2024;14:924.

[15] Maghsoudi K, Vazirinasab E, Momen G, Jafari R. Icephobicity and durability assessment of superhydrophobic surfaces: The role of surface roughness and the ice adhesion measurement technique. Journal of Materials Processing Technology 2021;288:116883.

[16] Lyu N, Shao Z, He H, Wang F, Liang C, Zhang X. Performance study of an active-passive combined anti-frosting method for fin-tube heat exchanger. Building and Environment 2022;222:109365.

[17] Shen Y, Wu Y, Tao J, Zhu C, Chen H, Wu Z, et al. Spraying Fabrication of Durable and Transparent Coatings for Anti-Icing Application: Dynamic Water Repellency, Icing Delay, and Ice Adhesion. ACS Appl Mater Interfaces 2019;11:3590–8.

[18] Machado C, Stern B, Huang H, Meem AUH, Huang J, Park K-CK. Robust hybrid diffusion control for long-term scalable frost prevention. Sci Adv 2024;10:eadq8525.

[19] Leoni A, Mondot M, Durier F, Revellin R, Haberschill P. Frost formation and development on flat plate: Experimental investigation and comparison to predictive methods. Experimental Thermal and Fluid Science 2017;88:220–33.

[20] Stendardo L, Gastaldo G, Budinger M, Pommier-Budinger V, Tagliaro I, Ibáñez-Ibáñez PF, et al. Reframing ice adhesion mechanisms on a solid surface. Applied Surface Science 2023;641:158462.

[21] Rønneberg S, He J, Zhang Z. The need for standards in low ice adhesion surface research: a critical review. Journal of Adhesion Science and Technology 2020;34:319–47.

[22] Work A, Lian Y. A critical review of the measurement of ice adhesion to solid substrates. Progress in Aerospace Sciences 2018;98:1–26.

[23] Yang K-S, Zheng J-W, Wu K-L, Wu Y-L. Performance of the frosting characteristics of fin-and-tube heat exchanger subject to superhydrophobic coating. Applied Thermal Engineering 2023;235:121338.